ELSEVIER

PII: S0032-3861(96)00982-2

Polymer Vol. 38 No. 16, pp. 4097–4101, 1997
© 1997 Elsevier Science Ltd
Printed in Great Britain. All rights reserved
0032-3861/97/$17.00 + 0.00

Analysis of two-stage crystallization kinetics for poly(ethylene terephthalate)/ poly(ether imide) blends

Jenn Chiu Hwang* and Chia-Chen Chen
Department of Chemical Engineering, Yuan Ze Institute of Technology, Nei-Li, Taoyuan, Taiwan, ROC

and Hsin-Lung Chen
Department of Chemical Engineering, Chang Gung College of Medicine and Technology, Kwei-San, Taoyuan, Taiwan 333, ROC

and Wen-Chung Ou Yang
Department of Chemical Engineering, National Kaohsiung Institute of Technology, Kaohsiung, Taiwan 807, ROC
(Received 25 June 1996; revised 12 September 1996)

Isothermal crystallization kinetics of poly(ethylene terephthalate) (PET) in its blends with poly(ether imide) (PEI) has been investigated by differential scanning calorimetry (d.s.c.). A modified Avrami analysis considering both primary and secondary crystallization was employed to extract the kinetic behaviour of these two crystallization stages. The crystallization rate constants at various crystallization temperatures (T_c) were obtained from the analysis for different PET/PEI blend compositions. A Hoffman–Lauritzen analysis was conducted for both primary and secondary crystallization. An average value of the nucleation constant $K_g \approx 2.89 \times 10^5$ was obtained from the analysis, and the fold surface free energy σ_e was then calculated to be 70.6 erg cm^{-2}. © 1997 Elsevier Science Ltd.

(Keywords: poly(ethylene terephthalate); poly(ether imide); crystallization kinetics)

INTRODUCTION

Poly(ether imide) (PEI) is an amorphous high performance polymer with a glass transition temperature (T_g) of 215°C. PEI has been found to form a miscible blend with poly(ethylene terephthalate) (PET) in the melt[1,2]. Because of the crystallizable nature of PET, PET/PEI blends are basically crystallizable in the temperature range between the melting point and T_g. The crystallization behaviour of PET/PEI blends has been characterized in a previous study[2]. Both degree of crystallinity and bulk crystallization rate of PET were found to decrease upon blending with PEI[2].

It is known that blending with an amorphous polymer may exert a dramatic effect on the thermodynamic and kinetic parameters governing the crystallization of the crystalline polymer[3–7]. Therefore, blending appears to be a useful route for controlling the crystallization rate of a crystalline polymer. In order to provide a systematic control of crystallization rate, it is essential for the crystallization kinetics of a polymer blend to be investigated in detail. In this paper, the bulk crystallization kinetics of PET/PEI blends are reported. A modified Avrami analysis considering both primary and secondary crystallization was employed to reveal the kinetic behaviour of these two crystallization stages. The effects of crystallization temperature and composition on the rates of these stages will be discussed.

EXPERIMENTAL

The PET sample used in this study was obtained from Goodyear Tire and Rubber Co., carrying the identification of Vituf. PEI was obtained from General Electric (GE, Ultem 1000), and its molecular weights were $M_n = 12\,000$ and $M_w = 30\,000$.

Blending of PET and PEI was carried out by solution precipitation. PET and PEI were dissolved in dichloroacetic acid at room temperature, yielding a 4 wt% solution. The blends were subsequently recovered by precipitating them in a tenfold excess volume of water. The blends were washed with a large amount of water and then dried *in vacuo* at 100°C for 5 days. It has been reported previously that PET/PEI blends as precipitated from dichloroacetic acid were not fully compatible, and about 15 min of annealing at 280°C was required to homogenize the blends[2]. Therefore, all the samples used in this study had been homogenized by melt-annealing in a d.s.c. at 280°C for 20 min under nitrogen atmosphere.

The isothermal crystallization kinetics of PET/PEI blends were investigated by a Perkin-Elmer DSC 7. For the crystallization temperature (T_c) higher than 180°C,

* To whom correspondence should be addressed

the sample was annealed at 280°C for 3 min to erase its previous thermal history. The sample was then rapidly cooled at ca. 160°C min^{-1} to the desired T_c where the isothermal crystallization exotherm was recorded. For the T_c lower than 180°C, the sample was annealed at 280°C for 3 min followed by quenching into liquid nitrogen. The sample was then heated at 200°C min^{-1} to the desired T_c and the crystallization exotherm was recorded.

RESULTS AND DISCUSSION

The relative crystallinity, $X_c(t)$, accumulated as of time t can be calculated from the crystallization exotherms recorded by d.s.c. The results can then be used to extract the kinetic information via the well-known Avrami analysis[8]. The Avrami equation reads

$$\ln\{-\ln[1 - X_c(t)]\} = \ln k_n + n \ln t \qquad (1)$$

where k_n is the crystallization rate constant and n is the Avrami exponent which is related to the mechanism of nucleation as well as the growth geometry. In this paper, as the rate constant is expressed with a subscript n, it means that the unit of the rate constant is $[\text{min}]^{-n}$ which is dependent on the value of n; otherwise, the rate constant is given by $k = k_n^{1/n}$ which has the unit of $[\text{min}]^{-1}$. Typical plots of the Avrami analysis are shown in *Figure 1* for PET/PEI 60/40 blend undergoing crystallization at different temperatures. The slopes of the linear portion give values of $n \approx 3$, which suggests an instantaneous nucleation with spherical growth geometry. The spherulite morphology of PET/PEI blends was confirmed from the four-leaf H_v pattern in a small-angle light scattering study[9]. Values of n close to 3 were also observed for other PET/PEI blend compositions.

As with many crystalline polymers, the Avrami plot exhibited a deviation from linearity at the late stage of crystallization (this portion is denoted as the 'secondary portion' in this paper). Such a deviation has been attributed to the occurrence of secondary crystallization. Several models have been proposed to modify the original Avrami theory with the inclusion of secondary crystallization[10-13]. In this study, a modified Avrami theory proposed by Price was adopted to analyse the kinetic data for PET/PEI blends[11]. The Price model treated the primary crystallization as the formation of spherulite and the secondary crystallization as crystallization taking place inside the spherulite. The expression of $X_c(t)$ in the Price model is given by[11]

$$X_c(t) = \int_0^t \left[1 - ce^{-k_s^m(t-\tau)^m}\right] n k_p^n \tau^{n-1} e^{-k_p^n \tau^n} d\tau \qquad (2)$$

where k_p and k_s are the rate constants with the unit of min^{-1} for primary and secondary crystallization, respectively; n and m are the exponents of the primary and secondary crystallization, respectively; and c is the total relative crystallinity developed in the secondary crystallization.

The rate constants k_p and k_s can be obtained by fitting the experimental data of $X_c(t)$ using equation (2). Following the procedure devised by Hsiao[14], the values of n and m were chosen as fixed parameters and the values of k_p, k_s and c were obtained by curve fitting. The value of n was obtained for each T_c and each blend composition from the slope of the initial linear portion in the Avrami plot, as shown in *Figure 1*. For the value of m, because of the spatial restrictions imposed by the primary crystals, the dimensionality of growth in secondary crystallization should be less than that in primary crystallization, i.e. $m < n$[14]. The value of one was chosen for m since the slope of the secondary portion in the Avrami plot was about this value for nearly all blend compositions and T_c investigated. The value of $m = 2$ was also considered in the curve fitting, but the values of k_p, k_s, and c obtained from the best fit using this value did not differ appreciably from that obtained using $m = 1$. However, $m = 1$ provided a better fit than $m = 2$. The initial value of k_p was obtained from the intercept of the initial linear portion in the Avrami plot; the initial value of k_s was calculated from the intercept by applying Avrami analysis to the secondary portion; and the initial value of c was obtained from one minus the relative crystallinity corresponding to the point where the Avrami plot started to deviate from the initial linearity. The curve fitting was performed using the Simplex method[15]. The reliability of the curve fitting was justified by comparing the fitted values of k_p with that obtained by Avrami analysis. If the fitted value of k_p differed appreciably from that obtained by the Avrami analysis, a new set of initial values for k_p, k_s and c was chosen and the curve fitting was reconducted.

Figure 2 compares the $X_c(t)$ calculated by the Price model (equation (2)) with that calculated by the Avrami equation (equation (1)) for PET/PEI 60/40 and 40/60 blends. *Table 1* tabulates the fitted values of k_p, k_s and c for three blend compositions. Generally speaking, the

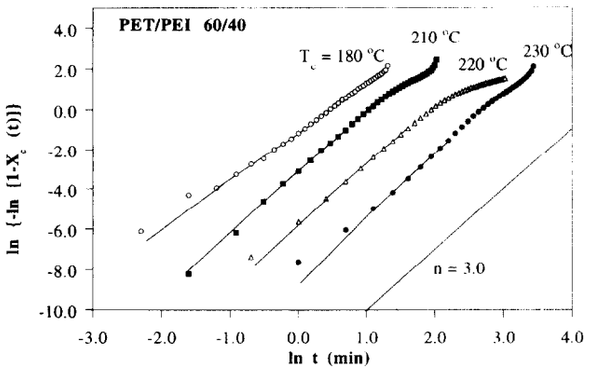

Figure 1 Avrami plot of PET/PEI 60/40 blend undergoing crystallization at different temperatures

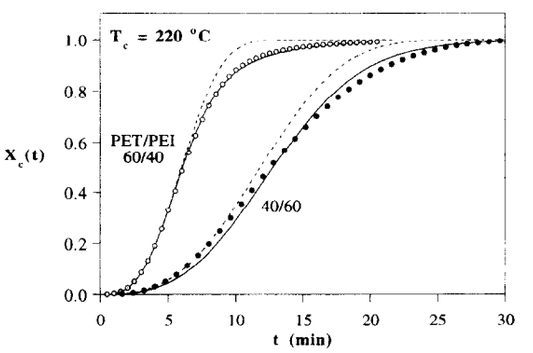

Figure 2 Comparison of $X_c(t)$ calculated by the Price model (solid line) with that calculated by the Avrami equation (dashed line) for PET/PEI 60/40 and 40/60 blends. Crystallization temperature was 220°C

values of c lie between 0.10 and 0.35, which is consistent with the suggestion by Hsiao[14]. *Figure 3* displays the plot of the logarithmic rate constants vs T_c. The temperature variations of the rate constants exhibit the conventional dumbbell shape, which is due to the interplay between the segmental mobility and the nucleation driving force that controls the rate of crystallization. The rate constants for pure PET and the 70/30 blend could not be determined over the entire T_c range because the crystallization proceeded too fast to be detected by d.s.c.

Table 1 Values of k_p, k_s and c obtained from the fit using the Price model for PET/PEI 100/0, 60/40 and 40/60 blends

PET/PEI	T_c (°C)	k_p (min^{-1})	k_s (min^{-1})	c
100/0	95	0.0331	0.1608	0.113
	100	0.1022	0.6030	0.150
	105	0.2338	0.7103	0.251
	110	0.6713	3.2567	0.227
	220	1.2300	4.9990	0.120
	225	0.6450	1.8339	0.282
	230	0.2633	1.0430	0.186
60/40	155	0.2149	0.2861	0.208
	165	0.4330	0.6632	0.274
	175	0.5407	2.0212	0.187
	185	0.8656	2.6605	0.104
	195	0.8861	3.8489	0.169
	205	0.7318	2.4500	0.102
	215	0.2552	0.7460	0.098
	225	0.1575	0.4419	0.154
40/60	190	0.0496	0.1590	0.197
	200	0.0950	0.2752	0.340
	205	0.0900	0.2803	0.301
	215	0.0864	0.1437	0.320
	220	0.0751	0.1861	0.272
	225	0.0210	0.2188	0.269

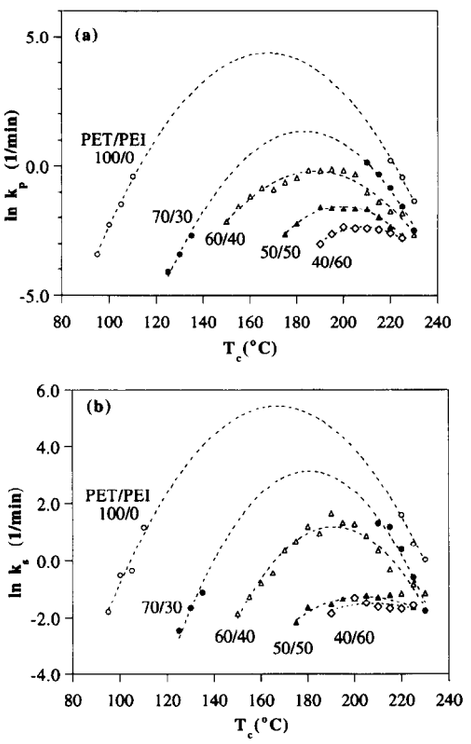

Figure 3 Temperature variations of (a) $\ln k_p$ and (b) $\ln k_s$ of PET/PEI blends. The curves of PET and 70/30 blends were obtained from second-power polynomials

It is seen that the rates of both primary and secondary crystallization decreased with increasing PEI composition in the blends.

Figure 3 also shows that for both primary and secondary crystallization the temperature at which the maximum crystallization rate is located, T_{max}, shifts to a higher value with increasing PEI concentration in the blends. The shift of T_{max} has been attributed to the change in T_g and the depression in equilibrium melting point (m.p.) upon blending. A reduced parameter, θ, has been introduced and, as the rate constants are plotted against θ, the value of θ where the maximum crystallization rate is located, θ_{max}, should be invariant with blend composition. θ is defined as[3]

$$\theta = \frac{T_c - T_g}{T^0_{mb} - T_g} \tag{3}$$

where T^0_{mb} is the equilibrium m.p. of the blend. The equilibrium M.P. of PET/PEI blends has been investigated previously, and it has been found that the m.p. depression is very small for this binary system because of fairly weak interaction between these two components[16]. This conclusion was also supported by the T_g–composition variation study[2]. Thus the equilibrium m.p. of pure PET (280°C) was taken as the value of T^0_{mb} for all PET/PEI blends in order to calculate θ. The T_gs of amorphous PET/PEI blends used to calculate θ are tabulated in *Table 2*. The plot of logarithmic rate constants vs θ is shown in *Figure 4*. It can be seen that, in contrast to *Figure 3*, θ_{max} is located at ca. 0.46 and is relatively invariant with blend composition. Since the depression of equilibrium m.p. is negligible for PET/PEI blends, the shift of T_{max} toward higher temperature with increasing PEI composition can be ascribed to the increase of T_g or to reduction in segmental mobility of PET upon blending with PEI. It is also noted that the T_{max} of primary and secondary crystallization is approximately the same for a given blend composition. This would suggest that the average melt compositions from which these two crystallization stages proceeded were approximately the same.

The previous study on PET/PEI blends has indicated the occurrence of liquid–liquid demixing on crystallization of this system[2]. This behaviour could influence the crystallization behaviour since the liquid–liquid demixing may shift the composition of the melt where the crystallization takes place. Nevertheless, this effect seems to be insignificant judging from the $\ln k$ vs θ plot in *Figure 4*. The θ parameter was calculated by equation (3) using the T_g associated with the initial melt composition, and, because θ_{max} is approximately invariant with blend composition, this would imply that the composition of the melt from which the crystallization proceeded was probably close to the initial melt composition.

Table 2 Glass transition temperatures (T_g) of amorphous PET/PEI blends

PET/PEI composition	T_g (°C)
100/0	77.1
70/30	95.1
60/40	114.8
50/50	130.6
40/60	149.2

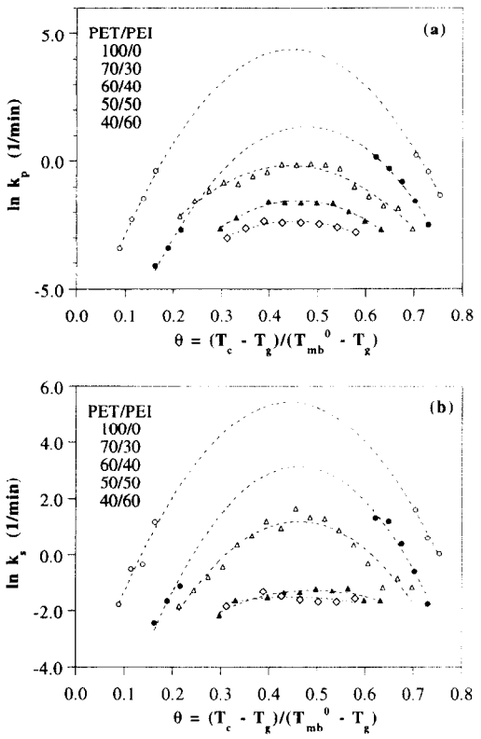

Figure 4 (a) $\ln k_p$ and (b) $\ln k_s$ vs θ plot of PET/PEI blends. The value of θ_{max} is relatively independent of blend composition

The crystallization rate constant is related to both the growth rate and the nucleation density. In this study, k_p is suggested to be associated with instantaneous nucleation with spherical growth geometry; thus k_p is given by[17]

$$k_p = \left(\frac{4\pi G_p^3 N_p}{3}\right)^{1/3} \tag{4}$$

where G_p is the growth rate and N_p is the number of nuclei per unit volume for primary crystallization, respectively. For the secondary crystallization, the value of $m = 1$ is attributed to instantaneous nucleation with rod growth geometry[17]. In this case k_s is expressed as

$$k_s = \pi R_0 G_s N_s \tag{5}$$

where G_s and N_s are the growth rate and nucleation density of secondary crystallization, respectively, and R_0 is the radius of the rod. Expressing equations (4) and (5) in logarithmic forms,

$$\ln k_p = \ln k'_{p0} + \ln G_p \tag{6}$$

$$\ln k_s = \ln k'_{s0} + \ln G_s \tag{7}$$

where k'_{p0} and k'_{s0} are constants. The growth rate formulated by Lauritzen and Hoffman has been modified by Boon and Azcue for polymer blends by considering an additional entropic contribution due to the decreased probability of selecting a crystalline sequence from the miscible melt[3]. This modification gives the growth rate as

$$\ln G = \ln G_0 + \ln \phi_2 - \frac{U^*}{R(T_c - T_0)} - \frac{K_g}{T_c(T_{mb}^0 - T_c)f} + \frac{\lambda \sigma T_{mb}^0}{b_0 \Delta h_f^0 (T_{mb}^0 - T_c) f} \ln \phi_2 \tag{8}$$

where G_0 is the pre-exponential constant; ϕ_2 is the volume fraction of PET; U^* is the activation energy required to transport the segments across the liquid–solid interface; T_0 is the temperature where such a transport ceases; $f = 2T_c/(T_{mb}^0 + T_c)$, a factor taking account of the temperature dependence of the enthalpy of melting (Δh_f^0); λ is a constant, $\lambda = 2$ for regimes I and III and $\lambda = 1$ for regime II growth; and K_g is a secondary nucleation constant given by

$$K_g = \frac{\alpha b_0 \sigma \sigma_e T_m^0}{k_B \Delta h_f^0} \tag{9}$$

where σ and σ_e are the side and fold surface free energy, respectively; b_0 is the monomolecular thickness; and α is a constant, $\alpha = 4$ for regimes I and III and $\alpha = 2$ for regime II growth.

Substituting equation (8) into equations (6) and (7) and rearranging terms,

$$\psi(k) = \ln k - \ln \phi_2 + \frac{U^*}{R(T_c - T_0)} - \frac{\lambda \sigma T_{mb}^0}{b_0 \Delta h_f^0 (T_{mb}^0 - T_c) f} \ln \phi_2 = \ln k_0 - \frac{K_g}{T_c(T_{mb}^0 - T_c)f} \tag{10}$$

where k can be k_p or k_s, and k_0 can be k_{p0} or k_{s0}. Equation (10) indicates that a plot of $\psi(k)$ vs $1/T_c(T_{mb}^0 - T_c)f$ should yield a straight line with the slope given by K_g. This analysis was applied to both primary and secondary crystallization. The universal values of $U^* = 1500\,\text{cal mol}^{-1}$ and $T_0 = T_g - 30$ were adopted here for both primary and secondary crystallization. These values have also been employed previously for the growth rate analysis of pure PET[18]. The values of other parameters for this analysis include: $\Delta h_f^0 = 2.09 \times 10^9\,\text{erg cm}^{-3}$, $b_0 = 5.53\,\text{Å}$, and $\sigma = 19.3\,\text{erg cm}^{-2}$ as evaluated from the characteristic ratio[19]. The value of λ was taken as unity, signifying a regime II crystallization for PET[18].

The plot of $\psi(k)$ vs $1/T_c(T_{mb}^0 - T_c)f$ is shown in *Figure 5* for 60/40 blend. It can be seen that the slopes for both primary and secondary crystallization are

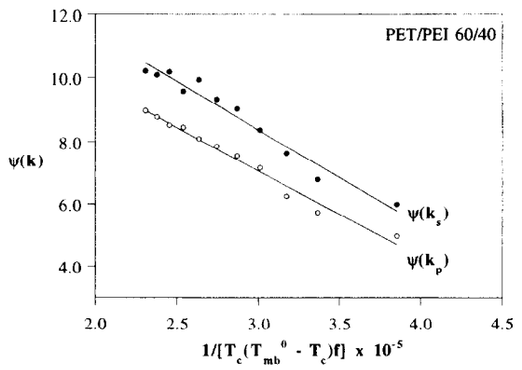

Figure 5 Plot of $\psi(k)$ vs $1/[T_c(T_{mb}^0 - T_c)f]$ for both primary and secondary crystallization of PET/PEI 60/40 blend

Tabele 3 Values of $\ln k_0$ and K_g obtained from the analysis of primary and secondary crystallization kinetics

	Primary crystallization		Secondary crystallization	
PET/PEI	$\ln k_0$	$K_g \times 10^{-5}$	$\ln k_0$	$K_g \times 10^{-5}$
100/0	15.47	3.03	16.77	3.04
70/30	15.72	3.00	18.52	3.45
60/40	15.36	2.77	17.45	3.03
50/50	15.01	2.58	15.69	2.69
40/60	16.01	2.48	18.02	2.80

approximately the same. *Table 3* lists the numerical values of K_g obtained for different blend compositions. The average value of K_g was 2.89×10^5. This value is in good agreement with those reported previously for PET[20]. The surface free energy product $\sigma\sigma_e$, calculated from equation (8) using this K_g value, was 1363 erg^2 cm^{-4} and hence the fold surface free energy σ_e was calculated to be 70.6 erg cm^{-2}.

CONCLUSIONS

A crystallization kinetic model considering both primary and secondary crystallization has been adopted to extract the crystallization rates of PET/PEI blends. It was shown that this model provided a better description of the experimental data than the conventional Avrami analysis. The primary and secondary crystallization rate constants at various T_cs were obtained from the analysis for different PET/PEI blend compositions. It was found that the rates of both crystallization stages decreased with increasing PEI composition. Because the temperature at which the maximum crystallization rate was located, T_{max}, was approximately the same for primary and secondary crystallization at a given blend composition, this suggests that the average melt compositions from which these two crystallization stages proceeded were about the same. The Hoffman–Lauritzen analysis was also applied for both primary and secondary crystallization. An average value of the nucleation constant $K_g \approx 2.89 \times 10^5$ was obtained from the analysis, and the fold surface free energy σ_e was then calculated to be 70.6 erg cm^{-2}.

ACKNOWLEDGEMENT

This work was supported by the National Science Council of the Republic of China under grant NSC 85-2216-E-182-002.

REFERENCES

1. Mart'inez, J. M., Eguiaz'abal, J. I. and Naz'abal, J., *J. Appl. Polym. Sci.*, 1993, **48**, 935.
2. Chen, H.-L., *Macromolecules*, 1995, **28**, 2845.
3. Boon, J. and Azcue, J. M., *J. Polym. Sci. Part A*, 1968, **6**, 885.
4. Wang, T. T. and Nishi, T., *Macromolecules*, 1977, **10**, 421.
5. Alfonso, G. C. and Russell, T. P., *Macromolecules*, 1986, **19**, 1143.
6. Chow, T. S., *Macromolecules*, 1990, **23**, 333.
7. Saito, H., Okada, T., Hamane, T. and Inoue, T., *Macromolecules*, 1991, **24**, 4446.
8. Avrami, M., *J. Chem. Phys.*, 1939, **7**, 1103.
9. Chen, H.-L., Hwang, J. C. and Chen, C. C., *Macromolecules*, submitted.
10. Hiller, I. H., *J. Polym. Sci. Part A*, 1965, **3**, 3067.
11. Price, F. J., *J. Polym. Sci. Part A*, 1965, **3**, 3079.
12. Hoshino, S., Meinecke, E., Powers, J., Stein, R. S. and Newman, S., *J. Polym. Sci. Part A*, 1965, **3**, 3401.
13. Velisaris, C. and Seferi, J., *Polym. Eng. Sci.*, 1986, **26**, 1574.
14. Hsiao, B. J., *Polym. Sci. Polym. Phys. Ed.*, 1993, **31**, 237.
15. Nelder, J. A. and Mead, R., *Computer J.*, 1965, **7**, 308.
16. Chen, H.-L., Hwang, J. C. and Chen, C. C., *Polymer*, 1996, **37**, 5461
17. Schultz, J. M., *Polymer Materials Science*. Prentice-Hall, Englewood Cliffs, 1974.
18. Runt, J., Miley, D. M., Zhang, K. P., Gallagher, K. P., McFeaters, K. and Fishburn, J., *Macromolecules*, 1992, **25**, 1929.
19. Medellin-Rodriguez, F. J., Philips, P. J. and Lin, J. S., *Macromolecules*, 1995, **28**, 7744.
20. van Antwerpen, F. and van Krevelen, D. W., *J. Polym. Sci. Polym. Phys. Ed.*, 1972, **10**, 2423.